



Characterisation of the weathered bedrock aquifer at the Rossdale Golf Club to assess the feasibility of ASR

Paul Pavelic, Peter J. Dillon, Peter G. Cook, Karen E. Barry and Joao Mimoso

September 2008

Smart Water Fund
REPRESENTED BY

City West Water
Melbourne Water
South East Water
Yarra Valley Water
Department of Sustainability and Environment



Australia is founding its future on science and innovation. Its national science agency, CSIRO, is a powerhouse of ideas, technologies and skills.

CSIRO initiated the National Research Flagships to address Australia's major research challenges and opportunities. They apply large scale, long term, multidisciplinary science and aim for widespread adoption of solutions. The Flagship Collaboration Fund supports the best and brightest researchers to address these complex challenges through partnerships between CSIRO, universities, research agencies and industry.

The Water for a Healthy Country Flagship aims to achieve a tenfold increase in the economic, social and environmental benefits from water by 2025. The work contained in this report is collaboration between CSIRO and Victorian Smart Water Fund, South East Water Limited, Southern Rural Water, Melbourne Water Corporation, Department of Sustainability and Environment, EPA, Department of Human Services, and Sinclair Knight Merz.

For more information about Water for a Healthy Country Flagship or the National Research Flagship Initiative visit www.csiro.au/org/HealthyCountry.html

Citation: Pavelic P, Dillon PJ, Cook PG, Barry KE and Mimoso, J, 2008. Characterisation of the weathered bedrock aquifer at the Rosssdale Golf Club to assess the feasibility of ASR. CSIRO: Water for a Healthy Country National Research Flagship.

Copyright and Disclaimer

© 2008 CSIRO To the extent permitted by law, all rights are reserved and no part of this publication covered by copyright may be reproduced or copied in any form or by any means except with the written permission of CSIRO.

Important Disclaimer:

CSIRO advises that the information contained in this publication comprises general statements based on scientific research. The reader is advised and needs to be aware that such information may be incomplete or unable to be used in any specific situation. No reliance or actions must therefore be made on that information without seeking prior expert professional, scientific and technical advice. To the extent permitted by law, CSIRO (including its employees and consultants) excludes all liability to any person for any consequences, including but not limited to all losses, damages, costs, expenses and any other compensation, arising directly or indirectly from using this publication (in part or in whole) and any information or material contained in it.

Cover Photograph:

Description: Downhole flowmeter testing of BH4 at the Rosssdale Golf Club, June 2006. Don Freebairn (DWLBC) is shown lowering the flowmeter and packer assembly down the well. Two reels containing the pressure delivery tubing and monitoring pump can be seen on the bottom RHS of the image.

Photographer: Paul Pavelic

© 2008 CSIRO

ACKNOWLEDGEMENTS

This work was made possible with the financial support of the Victorian Smart Water Fund through the auspices of the 'Developing Aquifer Storage and Recovery Opportunities in Melbourne' Project. The authors gratefully acknowledge the Project Steering Committee comprised of representatives from Smart Water Fund, South East Water Limited, Southern Rural Water, Melbourne Water Corporation, Department of Sustainability and Environment, EPA, Department of Human Services, CSIRO Water for Healthy Country Flagship, CSIRO Land and Water and Sinclair Knight Merz.

The following individuals are thanked for their assistance over the course of the investigation:

- Stephen Parsons and Robert Molloy (Sinclair Knight Merz) for coordinating the collection of core material and logistical support during the field campaigns
- Paul Kortholt (Rossdale Golf Club) for site access and field assistance
- Don Freebairn and Brian Traegar (SA Department of Water, Land and Biodiversity Conservation) for undertaking geophysical testing
- Duncan Cogswell (Borehole Wireline Pty Ltd) for processing of the ATV data
- Mark Raven (CSIRO Mineralogical and Geochemical Services Group) for performing XRD analyses on core samples
- John Dighton, Michelle Caputo and Megan Lefournour (CSIRO Land and Water) for guidance with the radon technique and analysis of samples
- Adrian Beech (CSIRO Land and Water Analytical Chemistry Unit) for physico-chemical analyses on core samples
- Heinz Buettikofer (CSIRO Land and Water) for drafting the location map in Figure 2.1
- Joanne Vanderzalm (CSIRO Land and Water) for providing advice in relation to clay dispersion

EXECUTIVE SUMMARY

The Rossdale Golf Club at Aspendale in Melbourne is the site selected for the Victorian Smart Water ASR Demonstration Project. The project aims to inject, store and recover urban stormwater via a confined weathered bedrock aquifer for the provision of irrigation supplies. This report documents the hydrogeological conditions at the Rossdale site from the viewpoint of assessing the risks in proceeding with an ASR pilot trial with respect to aquifer erosion, well collapse, clay dispersion, clogging of fractures and poor recoverability of the injected water.

The characterisation effort was conducted on two investigation wells at depths of up to 150 m and involved the use geophysical logging, downhole EM flowmeter logging, radon and temperature gradient profiles along with physico-chemical analyses on core samples.

The results show that the target aquifer is defined by small fracture apertures, relatively high matrix porosities and low matrix permeability. In light of the apparent moderate degree of variability in relative hydraulic conductivity profiles, and the general absence of distinct signatures in the temperature gradient and radon concentration profiles, it would appear that the aquifer exhibits either a low degree of aquifer heterogeneity, or more likely, high heterogeneity at a scale less than that of the measurements.

Although ASR into the weathered bedrock aquifer would not be without risk, these findings suggest that a pilot trial could proceed with caution at injection rates of around 0.5 L/s, initially utilizing water treated to potable standards. The most productive of the two investigation wells would function as the ASR well whilst the other would serve as an observation well.

CONTENTS

1.	Introduction	1
2.	Hydrogeological Setting	1
3.	Characterisation Methods	4
3.1.	Geophysical Logging	4
3.2.	Radon-222 Profiles	4
3.3.	Analyses on Intact Core and Disturbed Samples	4
3.4.	Aquifer Pump Testing	5
4.	Results	5
4.1.	Analysis of Core Samples	5
4.1.1.	General observations	5
4.1.2.	Physico-chemical analyses	6
4.1.3.	Clay dispersion tests	8
4.2.	Conventional Geophysical Logging	11
4.2.1.	Calliper	11
4.2.2.	Gamma	11
4.2.3.	Neutron	12
4.2.4.	Density	12
4.2.5.	Resistivity	12
4.2.6.	Groundwater EC	12
4.2.7.	Groundwater temperature	12
4.3.	Downhole Electromagnetic Flowmeter (EMF) Logging	15
4.3.1.	Principles of the EMF	15
4.3.2.	Field testing	15
4.3.3.	EMF Results	15
4.3.4.	K/K_{ave} profiles	16
4.3.5.	Comparison between the well yield testing during drilling and EMF data	16
4.3.6.	Estimated fracture apertures from EMF data	17
4.4.	Acoustic Televiewer Logs	18
4.5.	Radon Profiles	18
4.6.	Well Stability	18
5.	Discussion	19
6.	Conclusions	20
7.	Recommendations	21
8.	References	21
	Appendix 1: Selection of photographic images	23

LIST OF FIGURES

Figure 2.1	(a) Map of the Melbourne area, (b) Google Earth (©2007) image of the Rosedale Golf Club and (c) photograph of the investigation site in June 2006 (wells BH3, BH4 and BH2 (completed in the Werribee Formation) and the stormwater retention dam)	3
Figure 4.1	Results of clay dispersion tests for the seven samples of aquifer material in the presence of four water types (sample details are given in Table 4.1). The shaded bars give the mean values are overlain by errors bars that give the standard deviations.	10
Figure 4.2	Composite geophysical logs for BH3	13
Figure 4.3	Composite geophysical logs for BH4	14
Figure 4.4	Caliper logs of BH3 well before and after well development (left), and the resultant difference in well diameter (right)	19

LIST OF TABLES

Table 2.1	Characteristics of the two test wells: BH3 and BH4 (adapted from Lennon <i>et al</i> , 2006)	2
Table 4.1	Mineralogy data for the six sub-samples from BH4 and one bulk sample from BH3	6
Table 4.2	Physico-chemistry data for the 6 sub-samples from BH4 and 1 bulk sample from BH3	7
Table 4.3	Porosity and bulk density data for three intact core sub-samples from BH4	7
Table 4.4	Composition of the different types of water used in the test.....	9
Table 4.5	Change in turbidity of the dispersed sample and the estimated proportion of aquifer sample mobilised during the test.....	11
Table 4.6	Comparison of percent flow contribution of BH3 between all well yields during drilling and EMF profile	17
Table 4.7	Calculated values of fracture aperture (b) from incremental transmissivities determined from flowmeter and pumping test data	17

1. INTRODUCTION

The Rossdale Golf Club, located at Aspendale in the south-eastern suburbs of Melbourne, is the site selected for the Victorian Smart Water ASR Demonstration Project. The project aims to store and recover urban stormwater via a fractured rock aquifer to provide irrigation supplies, and is the first project of its kind planned for Victoria.

Characterisation of the fluid flow properties of the target aquifer is fundamental to the development of ASR schemes. Fractured rock aquifers are, by definition, inherently heterogeneous, and this hydrogeological complexity makes characterisation a challenge. It is now clearly recognized that heterogeneity plays a major role in influencing rates of movement and mixing of the injected water with the (usually more saline) ambient groundwater, which in turn controls the salinity of the water that is recovered. Further, the size, distribution and connectivity of fractures intersecting the well plays a major role in determining the extent of permeability reductions due to clogging processes, and dictates the pre-treatment requirements for the stormwater to achieve sustainable rates of injection.

The objective of this study is to evaluate the suitability of the target aquifer at the Rossdale site for ASR to determine the level of risk associated with excessive well clogging or unacceptably low recovery efficiencies. The hydrogeological conditions at the Rossdale site are determined by applying a variety of conventional and novel geophysical and hydrogeological techniques to two investigation wells. This report describes the results of the characterisation effort, and from this, the implications for proceeding with the ASR trial in the target aquifer.

2. HYDROGEOLOGICAL SETTING

The target aquifer is the weathered bedrock of Silurian age, encountered at depths of between 77 and 81 m and extending to a depth of >146 m at the study site (Lennon *et al*, 2006). The aquifer consists of interbedded sandstones and siltstones with sub-vertical bedding planes. Siltstone is more prevalent than sandstone. Generally, the primary porosity of the aquifer is thought to be of low permeability, however secondary features such as bedding planes and fractures impart secondary porosity that can lead to higher permeability and result in modest well yields (Whiting, 1967; Leonard, 1992).

Regionally, the structure of the Silurian bedrock formation resembles a tight, concertina-type folding pattern, with a general strike direction of NNE (Whiting, 1967). The nearest major fault is the Selwyn fault, situated around 10km south of the study site (Lennon *et al*, 2006).

This aquifer was chosen as the target for ASR after previous drilling at the Rossdale site into the overlying Werribee Formation identified that aquifer to be thinner and of lower yield than expected, and consequently, unsuitable for ASR (Lennon *et al*, 2006).

The two investigation wells, BH3 and BH4, were drilled in December 2005 and June 2006 to depths of 127 m and 146 m, respectively (Table 2.1). Both wells were completed as open-hole (i.e. without a screen), with open intervals of 34 and 43 m respectively (Table 2.1). They are located near the south-eastern boundary of the Rossdale Golf Club, only 11 m apart and approximately 1 km from Port Phillip Bay (Figure 2.1). BH4 was drilled to greater depth and completed over a larger open interval than BH3 in the expectation that a greater well yield would result from intersecting a higher number of fractures (Table 2.1). It is intended that the most suitable investigation well be used for ASR and the other serve as an observation well. The aquifer is confined with transmissivities ranging from 1.2–1.4 m²/day. A reliable estimate of storage coefficient could not be obtained from the pump test analysis. The depth to standing water level is shallow (1.1–1.3m). Regional hydraulic gradients are believed to be towards Port Phillip Bay (Leonard, 1992) and subdued due to proximity to the sea and minimal pumping from the aquifer. The ambient groundwater is of brackish quality (2400–2700 μS/cm).

Table 2.1 Characteristics of the two test wells: BH3 and BH4 (adapted from Lennon *et al*, 2006)

Characteristic	BH3	BH4
Date drilling completed	2 December 2005	2 June 2006
Location (Northings & Eastings)	5,789,197 N; 334,666 E	5,789,192.5 N; 334,656 E
Total drilled depth below ground surface (bgs)	127 m	146 m
Cased interval / Internal diameter	0–93 m / 150 mm	0–103 m / 140 mm
Open interval: as drilled / on 23 June 2006*	93–127 m / 93–123.5 m	103–146 m / 103–117 m
Drilled diameter of uncased interval	125 mm	125 mm
Well yield	1.25 L/sec	1.1–1.2 L/sec
Transmissivity	1.4 m ² /day	1.2 m ² /day
Storage coefficient	unreliable	unreliable
Groundwater EC	2400–2700 µS/cm	2400–2700 µS/cm
Depth to standing water level (21–22 June 06)	1.32 m	1.13 m

* well reamed on 23 June 2006 to address slumping, see section 4.6



Figure 2.1 (a) Map of the Melbourne area, (b) Google Earth (©2007) image of the Rosedale Golf Club and (c) photograph of the investigation site in June 2006 (wells BH3, BH4 and BH2 (completed in the Werribee Formation) and the stormwater retention dam)

3. CHARACTERISATION METHODS

3.1. Geophysical Logging

Downhole geophysical logging was performed on BH3 and BH4 by the Geophysical Technical Services section of the SA Department of Water, Land and Biodiversity Conservation on 21 and 22 June 2006. The suite of logs performed on each well included three-arm caliper, natural gamma, neutron, density, resistivity, fluid electrical conductivity (EC), fluid temperature, electromagnetic flowmeter (EMF) and acoustic televiewer (ATV). On 23 June caliper logging was repeated for BH3, immediately after a reaming operation had been performed earlier that day to address the slumping observed during the initial logging runs. The other logs were not repeated as reaming had failed to restore BH3 to its original depth and suggested the lower section of the well was potentially unstable.

3.2. Radon-222 Profiles

Radon-222, a radioactive noble gas, is relatively ubiquitous in groundwater since it is derived from radioactive decay of uranium-series isotopes that are commonly found in aquifer materials. Measurement of the concentrations of radon within diffusion chambers positioned at varying depths within a well offers a method of estimating the relative groundwater flow rate since the relatively short half-life of radon (3.8 days) provides a sensitive measure of groundwater flow. An abundance of radon tends to be indicative of rapid throughflow whilst depletion of radon due to natural decay indicates reduced throughflow (Cook *et al*, 1999; Cook, 2003).

Two clusters of 50 mL diffusion chambers filled with radon-free deionized water were lowered into the open interval of BH3 and BH4 on a stainless steel trace at 2 m spacings on the afternoon of 23 June. Chambers remained undisturbed until their retrieval 66 days later on 28 August. Over the elapsed time period within the well the isotopic composition of the fluid within the chamber would have fully equilibrated. At equilibration, the concentration of radon-222 within the chamber, would have reached only 66% of the value of the local groundwater within the well due to the time taken for exchange to occur across the membrane (Cook *et al*, 2006).

Recovery of chambers from BH3 revealed that the upper section of the trace had become severely entangled leading to a reduction in the monitored depth range from 26 m to 13.1 m. This is suspected to have been caused by one or more chambers becoming temporarily caught on a protrusion from the well-face during the initial descent (see Appendix 1, Section C). The actual depths of the chambers were corrected from the chamber positions following recovery. Note that the cluster in BH4 were recovered without such incident (Appendix 1C).

Using the procedure outlined by Cook *et al*, (2006), 14 mL sub-samples were collected by syringe directly from each chamber and transferred to pre-weighed 22 mL Teflon-coated PTFE scintillation vial containing 6 mL Packard NEN mineral oil and transported overnight to the CSIRO Isotope Analytical Service in Adelaide. Radon data was corrected for the time-lag between collection and analysis and was adjusted to account for diffusive exchange across the membrane since differences in relative activity were the primary interest.

3.3. Analyses on Intact Core and Disturbed Samples

During drilling of BH4 intact cores of aquifer material were collected by Sinclair Knight Merz (SKM) between 102.8 and 110.5 m bgs using a HQ (63.5 mm diameter) core barrel (Lennon *et al*, 2006). In total, 5.8 m of core was recovered from the 7.7 m cored interval (75% core recovery). Recovered core samples were logged, photographed, wrapped in cling wrap then placed in air-tight PVC tubes by SKM and transported to CSIRO, Adelaide for analysis.

Six sub-samples from the BH4 cores were chosen to reflect the variability observed in the lithological, hydraulic conductivity and gamma logs. An aggregate sub-sample of sediment recovered during the BH3 reaming operation described earlier was also collected. A range of physico-chemical and mineralogical properties were tested on all seven sub-samples as follows:

- quantitative XRD analysis was performed by the CSIRO Mineralogical and Geochemical Services Group on a ground, 1 g sub-sample using a Philips PW1710 microprocessor-controlled diffractometer and the software package SIROQUANT
- electrical conductivity 1:5 soil:water ($EC_{1:5}$), pH 1:5 soil:water ($pH_{1:5}$) as well as with 0.01M $CaCl_2$ ($pH_{0.01M\ CaCl_2}$), organic carbon (OC), calcium carbonate ($CaCO_3$), exchangeable cations and cation exchange capacity (CEC) were determined by the CSIRO Land and Water Analytical Chemistry Unit
- particle size distributions were determined on sub-samples that were oven-dried, ground, and the >2 mm fraction removed. The sand fractions were characterised using sieves ranging in size from 53 μm to 2 mm. The silt and clay contents were calculated from suspension settling tests based upon Stokes' Law.
- clay dispersion tests with four types of water using the 'Emerson' method (detailed methods given in section 4.1.3)

In addition, three intact sub-samples, ranging in effective lengths from 6 to 10 cm, were chosen for analysis of total porosity and dry bulk density. Porosity was derived from the measured total water loss determined by oven drying overnight at 105 °C and bulk volume determined from the volumetric displacement of water. Bulk density was derived from the ratio of the oven-dry mass to the bulk volume.

Photographic images of the eight core tubes are given in Appendix 1A. The intervals identified for sub-sampling are indicated. Geological and geophysical logs for the core samples are given in Lennon *et al*, (2006).

3.4. Aquifer Pump Testing

SKM performed step- and constant rate discharge- testing of both investigation wells (Lennon *et al*, 2006). The test results are used in this report.

4. RESULTS

4.1. Analysis of Core Samples

4.1.1. General observations

Core logging by Lennon *et al* (2006) indicates that the bedrock aquifer is comprised of approximately 75% siltstone and 25% sandstone. The aquifer generally became less weathered/easily eroded and more competent with depth, although less competent sections are also encountered in the lower sections (refer to section 4.6). The sandstone was more highly fractured than the siltstone, with the latter having few (if any) fractures. The fractures were generally quite fine and closely spaced, although in places larger fractures were observed. In terms of strength, Lennon *et al* (2006) found the material ranged from relatively weak (i.e. "easily broken by hand") to moderate ("broken by hand with difficulty"), with the latter being more dominant. Breakup of the core material was usually possible by applying manual force along bedding planes and the cleavage planes oriented approximately orthogonal to the bedding planes.

The core samples suggest that the greater proportion of groundwater throughflow will be derived from the sandstone, however this generalization neglects the contribution from bedding and cleavage planes.

The cores were typically grey to black in colour, indicating the presence of organic matter (Blatt *et al*, 1980), and verified by the data presented in Table 4.2. Bedding plane surfaces were frequently associated with 'speckled' deposits, characteristic of pyrite, and in-filled with light coloured clays thought to be kaolin.

4.1.2. Physico-chemical analyses

The mineralogical composition data presented in Table 4.1 shows that the target aquifer is dominated by quartz, SiO₂ (48–73%), with lesser amounts of kaolin, Al₂Si₂O₅(OH)₄ (13–23%) and muscovite, KAl₂(AlSi₃O₁₀)(F,OH)₂ (7–18%), and trace amounts of siderite, FeCO₃ (0–11%), and chlorite, (Fe,Mg,Al)₆(Si,Al)₄O₁₀(OH)₈ (0–6%) and pyrite, FeS₂ (0.3–1.3%). Sandstone samples are associated with higher levels of quartz (>70%) and lower levels of kaolin (<20%), muscovite (<10%) and siderite (<2%). Chlorite is a silicate mineral commonly present in igneous rocks that does not contain chloride, and so would not detract from the use of chloride as a tracer of the injected water during an ASR trial (the name apparently originates from the Greek word for green).

The mineralogical characteristics of the bulk sample from BH3 are largely intermediate to the BH4 core sub-samples, suggesting a mix of sandstone and siltstone in the extracted sediment. During reaming, distinctive brassy-yellow cubic crystals characteristic of pyrite were clearly evident within the recovered sediment (Appendix 1B).

Table 4.1 Mineralogy data for the six sub-samples from BH4 and one bulk sample from BH3

Sample No.	Well	Depth (m bgs)	Lithology	Quartz (%)	Muscovite (%)	Kaolin (%)	Siderite (%)	Pyrite (%)	Orthoclase (%)	Chlorite (%)
1	BH4	103.85 ^A	sandstone	72	8	15	1	0.9	3	-
2	"	104.2 ^A	sandstone	70	7	19	-	1.3	2	-
3	"	107.45 ^A	siltstone	48	18	23	2	0.3	4	5
4	"	108.3 ^A	siltstone	50	13	18	11	1.2	4	3
5	"	109.15 ^A	sandstone	73	7	13	-	0.7	3	3
6	"	109.8 ^A	siltstone	51	16	21	<1	1.0	5	6
7	BH3	93-124 ^B	sandstone & siltstone	61	12	19	1	1.3	4	2

^A core sample from BH4
^B bulked sample from reaming of BH3

Table 4.2 Physico-chemistry data for the 6 sub-samples from BH4 and 1 bulk sample from BH3

Sample No.	Depth (m bgs)	Lithology	EC _{1:5} (dS/m)	pH _{1:5}	pH _{0.01M} CaCl ₂	OC (%)	Exch. Cat. _{TOT} cmol(+/-)/kg	CEC cmol (+-)/kg	CaCO ₃ (%)	d ₅₀ (µm)
1	103.85	sandstone	0.14	8.6	7.9	0.13	1.6	1.5	<0.5	106–180
2	104.2	sandstone	0.17	8.5	7.9	0.12	2.4	2.2	<0.5	180–250
3	107.45	siltstone	0.23	8.8	8.2	0.70	3.8	3.2	<0.5	500–1000
4	108.3	siltstone	0.17	9.1	8.3	0.48	4.6	4.0	1.5	250–500
5	109.15	sandstone	0.19	8.8	8.1	0.14	4.4	4.1	<0.5	250–500
6	109.8	siltstone	0.13	8.9	8.0	0.21	3.5	3.8	<0.5	250–500
7	93–124	sandstone & siltstone	0.31	7.6	7.2	0.23	3.9	3.7	<0.5	250–500

The physico-chemical properties of the six core sub-samples and one bulk sample are presented in Table 4.2. Samples described as siltstone are substantially higher in OC, marginally higher in pH, and generally higher in CEC and exchangeable cations. CaCO₃ was detected at trace amounts in only one sample (sample 4, siltstone, 108.3 m depth). Particle size data, although presented, are ambiguous because of the observed dependence of the effective grain size on the intensity of grinding.

Table 4.3 shows that the total porosity and bulk density are remarkably consistent between the three samples. Porosities were consistently 22–23%. Since there was no visible evidence of fractures on the three test cores, the measured values are considered representative of the porosity of the aquifer matrix. These results do not conform with the view that the basement rocks are of low porosity (Leonard, 1992).

The measured bulk densities from cores of 2.3–2.4 g/cm³ are marginally higher than the geophysical log inferred values of 2.0–2.2 g/cm³ at identical depths (refer to section 4.2).

Table 4.3 Porosity and bulk density data for three intact core sub-samples from BH4

Well	Depth (m bgs)	Lithology	Porosity (%)	Dry bulk density (g/cm ³)
BH4	103.7	sandstone	22	2.33
BH4	107.6	siltstone	23	2.31
BH4	109.2	sandstone	22	2.36

4.1.3. Clay dispersion tests

Deterioration in the hydraulic properties of an aquifer may occur during ASR as a result of clay dispersion (movement of interstitial clay particles) or clay swelling, when the solid phase is exposed to water of a different ionic strength. Aquifers that exhibit this tendency are described as being 'water sensitive' (Brown and Silvey, 1977). Clay dispersion and swelling arise from cation exchange reactions between ions in solution and those associated with the clays within the aquifer, and is known to be most prevalent where reactive clay minerals are present (particularly montmorillonite); where there is a large decrease in the salinity of the injected water compared to the ambient groundwater; and where the sodium adsorption ratio (SAR) of the recharge water is greater than that of the pore-water (Brown and Silvey, 1977; Gray and Rex, 1990; Scheuerman and Bergersen, 1990; Konikow *et al*, 2001). The exchange of divalent calcium and magnesium ions with monovalent sodium ions strengthens the ionic 'double layer' around clay particles and tends to prohibit the clustering of clay particles and encourage clay dispersion. Dispersion is probably more serious than swelling since it results in the physical movement and repacking of clay particles within the aquifer, and is thus largely irreversible.

Methods

Laboratory tests were performed to assess the potential for various types of potential ASR source waters to cause clogging of the clay minerals within the Silurian aquifer due to dispersion using the 'Emerson' method reported by Standards Association of Australia, (1980). Briefly, the approach relies on applying replicate batch tests of solid and liquid mixtures to characterize dispersion by measuring the increase in the turbidity of the supernatant, relative to that of the water (i.e. in the absence of solids).

Batch tests were performed to test the reactivity of the seven samples previously discussed in section 4.1.2. Sub-samples were oven-dried at 45 °C and homogenized by hand grinding to ensure uniformity of solid media replicates.

Four types of water were tested: 1) mains (tap) water, 2) stormwater, 3) ambient groundwater and 4) distilled water. Mains water, collected from the Rossdale site, was selected since any ASR testing would be expected to initially utilize this water source. Stormwater was obviously selected as it is the primary source water for ASR, whilst ambient groundwater was selected since it represents the baseline conditions within the aquifer. Distilled water, due to the very low concentration of solutes, was selected to mimic reverse osmosis pretreatment of stormwater which would reflect a worst-case scenario for injection.

100 mL of water was added to beakers containing a 0.6 g sub-sample of aquifer material in each. Three replicate beakers were prepared for each sediment-water combination. A beaker that contained only water was used as a control for each of the four water types. The turbidity of the solution was measured after a period of 48 hours to ensure that equilibrium conditions had established.

The composition of the waters are shown in Table 4.4. Electrical conductivities ranged from 21 $\mu\text{S}/\text{cm}$ for the distilled water through to 2850 $\mu\text{S}/\text{cm}$ for the groundwater with a sodium adsorption ratio (SAR) ranging from 0.6 for mains water to 14.9 for groundwater (SAR was not determined for the distilled water).

Table 4.4 **Composition of the different types of water used in the test**

Analyte	Distilled water	Mains water	Stormwater	Groundwater
Na ⁺ (mg/L)	N/A	5.5	56	465
Ca ²⁺ (mg/L)	N/A	4.7	21	88.5
Mg ²⁺ (mg/L)	N/A	1.5	6.6	27.1
K ⁺ (mg/L)	N/A	<1	5.9	5.5
SAR	N/A	0.6	2.7	14.9
EC (µS/cm)	20.5 ^A	118.3	575	2850
pH	6.6	6.51	7.53	7.29
Temp (°C)	22	22.2	22.1	22.1
Eh (mV)	274	270	190	176
DO (mg/L)	5.3	5.8	5.9	5.5
^A Milli-Q water used that was allowed to stabilize prior to test, thereby allowing enrichment of ionic strength due to atmospheric exchange				

Results

Values of turbidity for each of the sediment-water solutions and control waters are presented in Figure 4.1. Values for the control waters ranged from 0.5–0.7 NTU compared with 0.8–8.4 NTU for the sediment-water solutions, indicating that the presence of aquifer material consistently produced higher turbidity waters. Values of turbidity were sufficiently low such that visible signs of clouding in the solutions was minimal in most cases (Appendix 1B).

Differences were observed between the behaviour of each of the aquifer samples. Dispersive behaviour was highest in sample #6 and lowest in sample #1. Turbidities for sample #7 were largely intermediate of the other samples, as expected for an integrated sample from the entire aquifer profile. Interestingly, broad lithological class alone was not a reliable indicator of dispersion. For example, both the low dispersion sample #1 and high dispersion #5 are broadly described as sandstones but have a three-fold difference in cation exchange capacity (CEC) values (Table 4.2).

The net dispersive potential of each water type can be expressed in terms of the increase in turbidity relative to the control. For any water type this increase could be approximately described from the CEC of the aquifer with linear correlation coefficients with respect to CEC that ranged from 0.37 for distilled water to 0.59 for groundwater. The slopes of this relationship offer a measure of the sensitivity of the water types to dispersion. The values of the slope obtained were: 1.1 for distilled water, 0.4 for mains water, 0.3 for stormwater and 0.3 for ambient groundwater. Thus the dispersive tendency of the waters can be ranked as follows: distilled water >> mains water > stormwater ~ ambient groundwater.

The measured turbidity increases are estimated to have caused between <0.01% and 0.26% of the solid phase to have dispersed into solution (Table 4.5). The hydraulic impacts of this degree of mobility are difficult to assess in the absence of column experiments. Substantial dispersion-related permeability declines have been reported for lab columns filled with sandy aquifer sediments with as little as 2% montmorillonite (Brown and Silvey, 1977; Konikow et al, 2001).

These authors found that the declines were inversely correlated to the chloride concentration of the source water.

In aquifers where significant clay dispersion is expected as a result of freshwater injection into more saline aquifers, Brown and Silvey (1977) showed that an initial pre-flush of calcium-chloride solution was successful in avoided the problem by increasing the availability of calcium ions on the surface of the clay minerals. The viability of this treatment over the longer term is unknown.

Previous dispersion tests using an identical experimental approach to that described here were performed on core samples from a brackish sandstone (and siltstone) aquifer with CEC values ranging from 1.8 to 29 cmol(+)/kg (Pavelic et al, 2001). Turbidity increases were found to be less than 0.5 NTU for distilled water and up to 10 NTU for the low salinity injectant. Although the greater dispersion of the injectant relative to the distilled water is in contrast to the findings of this study, differences between the two studies are apparent. The CEC values in the previous study were typically higher than values reported here of 1.5–4.1 cmol(+)/kg, which is consistent with the presence of higher CEC smectites (montmorillonite) in the previous study. The salinity contrast between the two waters tested in the previous study was significantly less than for this study (<80 $\mu\text{S}/\text{cm}$ cf 2800 $\mu\text{S}/\text{cm}$). The previous study was equilibrated with similar ambient groundwater EC (2400 $\mu\text{S}/\text{cm}$) but substantially lower SAR (~4) than the present study. The SAR value of ~2 for the injectant in the previous study was similar to the present study.

If the dispersion-induced turbidity increase is assumed to relate to permeability decline, then this study shows a trend between clogging and salinity, as was found by Konikow *et al* (2001). This does not, however, concur with the findings of the study by Pavelic *et al* (2001) due, presumably, to the differences in the concentration and types of cations in the source and receiving waters, as well as the higher potential reactivity of the aquifer minerals, that are constrained by their initial equilibrium with lower SAR groundwater.

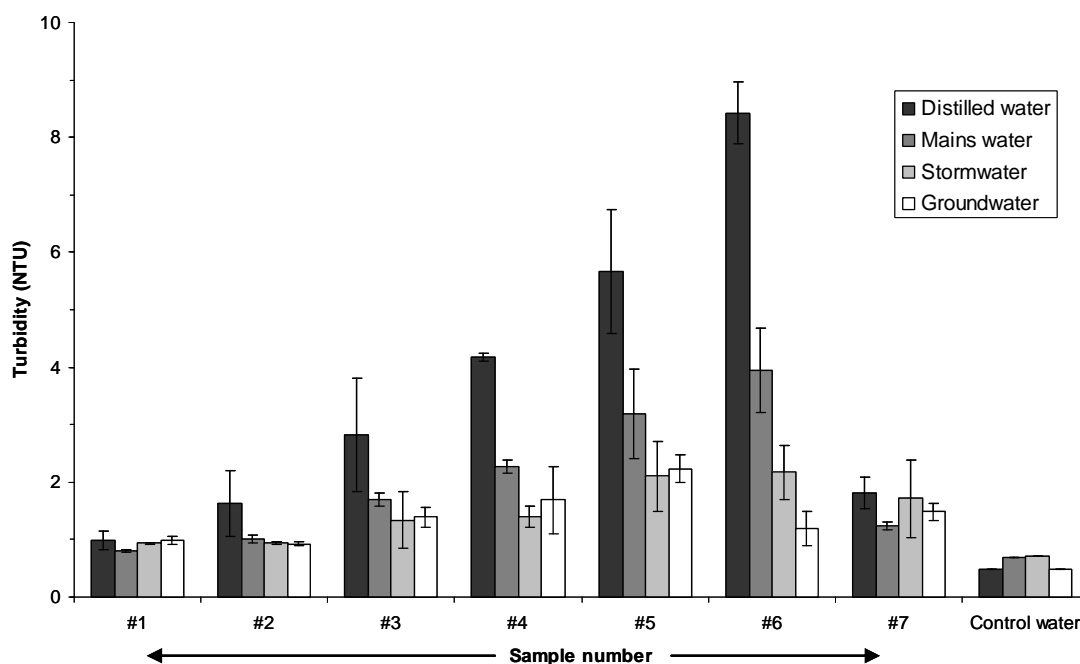


Figure 4.1 Results of clay dispersion tests for the seven samples of aquifer material in the presence of four water types (sample details are given in Table 4.1). The shaded bars give the mean values are overlain by errors bars that give the standard deviations.

Table 4.5 Change in turbidity of the dispersed sample and the estimated proportion of aquifer sample mobilised during the test

Water Type	EC ($\mu\text{S/cm}$)	Δ Turbidity ^A (NTU)	Dispersed portion of aquifer sample ^B (%)
Distilled water	20.5	0.5 – 7.9	0.02 – 0.26
Mains water	118	0.1 – 3.3	<0.01 – 0.11
Stormwater	575	0.2 – 1.5	0.01 – 0.05
Groundwater	2850	0.4 – 1.7	0.01 – 0.06

^A turbidity of sediment:water value minus the control value
^B estimated from ‘ Δ turbidity’ using TSS vs turbidity relationship

4.2. Conventional Geophysical Logging

The following descriptions are drawn from the composite geophysical plots presented in Figures 4.2 and 4.3. Data are presented with respect to the depth below the local ground surface elevation. The difference in elevation between the two wells was determined by surveying to be 0.29 m, with BH3 situated on slightly higher ground than BH4.

4.2.1. Calliper

Calliper log data indicates that the average effective diameter of BH3 ranged from 145 to 215 mm; values similar to, or greater than, the internal diameter of the casing. For BH4, the corresponding range was from 130 to 150 mm below 104.2 m bgs. The top 1 m of the open interval of BH4 was of distinctly larger diameter (up to 360 mm), presumably as a result of the rotary mud drilling and casing installation procedure (i.e. to allow for fluid recirculation during pressure cementing of the casing). Some minor slumping causing partial blockage of the open-hole was evident directly beneath this zone at a depth of around 104 m.

The total depth of BH3 on 20 June 2006 was 117.1 m bgs; 9 m less than the total depth of completion. For BH4 the depth was 116.7 m bgs; a shortfall of 29 m. Slumping reduced the open interval by approximately 30% for BH3 and 70% for BH4, thus denying the opportunity to log the lower portions of both wells.

In strongly cemented ‘hardrock’ formations, calliper logs are often used to identify the locations of fractures (e.g. Hess, 1986; Muldoon and Bradbury, 2005). However, for this variably cemented and highly weathered aquifer, the cavity features evident throughout the profiles appear to be unrelated to the presence or absence of fractures, and most probably represent the most easily eroded layers within the aquifer that contribute most to the sediment recovered during well development.

4.2.2. Gamma

Gamma ray logs are indicative of clay content and are hence useful for defining changes in lithology. In this setting lower counts are indicative of lower clay content (i.e. a tendency towards sandstone) and higher counts are indicative of higher clay contents (i.e. a tendency towards siltstone). Average values vary from 90 to 160 API in BH3 and from 100 to 160 API in BH4. Zones most clearly suggestive of sandstone occur at around 100–102 m and 114–115 m for BH3, and 103–105 m for BH4.

4.2.3. Neutron

Neutron logs are indicative of the total porosity and clay content (since clays contain bound water). Higher counts are indicative of lower porosity. Greater variability is observed in BH3 than BH4, with average values ranging from 200 to 350 CPS in BH3 and from 200 to 450 CPS in BH4. Zones with lowest porosity and thus most suggestive of sandstone, occur at around 100, 114, 116 and 117 m for BH3, and 105 and 115 m for BH4. This partly agrees with inferences drawn from the gamma log.

4.2.4. Density

Densities range from 1.7 to 2.2 g/cm³ for BH3 and from 1.9 to 2.3 g/cm³ for BH4. Distinct declines in density at 101 m in BH3 and 103 m for BH4 are indicative of void space observed in caliper logs, and possibly the presence of major fractures.

4.2.5. Resistivity

Electrical resistivity logs are indicative of the combined effect of matrix and fluid resistivity. Values range from 50 to 170 Ohm/m for BH3 and from 100 to 200 Ohm/m for BH4. Note that perturbations at the uppermost interval of BH4 reflect variations in well diameter. Given the uniformity of fluid conductivities (see section 4.2.6), the variability must be largely ascribed to variations in matrix resistivity.

4.2.6. Groundwater EC

Downhole EC profiling indicates consistent values of around 2900 $\mu\text{S}/\text{cm}$ in both test wells. The uniformity in EC with depth contrasts with changes of up to 300 $\mu\text{S}/\text{cm}$ observed by Lennon *et al* (2006) during aquifer pump testing of BH3 and BH4. Groundwater drawn from the more permeable zones of the aquifer during pumping may differ in EC to that measured within the open-hole during ambient conditions. The relative uniformity in the vertical EC profile contrasts with the core EC_{1.5} values that varied by a factor of 2 or more, which agrees with the mechanism proposed.

4.2.7. Groundwater temperature

Groundwater temperatures steadily increase with depth as a result of the geothermal gradient from 18.6 °C at 93 m to 19.3 °C at 117 m bgs at an average rate of 0.029 °C/m. Temperature profiles for BH3 and BH4 are consistent.

Subtle perturbations in the thermal gradient over specific depth intervals have been shown to be reflective of the presence of hydraulically active fractures in uncased wells (e.g. Cook *et al*, 1999). The technique was initially applied to the data with poor results due to the relatively low sensitivity of the Hydrolab MS4A sonde used (0.01 °C resolution; 0.1 °C accuracy), even when the integration range was increased from 0.1 m to 1 m intervals.

Temperature measurements were repeated on 28–29 August 2006 using a Seabird SBE 39 sonde, an instrument with a resolution of 0.004 °C. The temperature gradient profiles, presented in Figures 4.2 and 4.3, reveal an oscillatory fluctuation pattern in both wells, with amplitudes that are typically <1m. Fluctuation ranges are typically ~0.15 °C/m for BH3 and ~0.2 °C/m for BH4.

Perturbations in excess of 0.1 °C/m appear not to be random noise associated with the accuracy of the instrument. They occur at five locations in BH3 at depths of 90.9 m, 98.8 m, 101–102 m, 104.0 m and 108.2 m and at four locations in BH4 at depths of 102.8 m, 105.1 m, 107.1 m and 115.2 m.

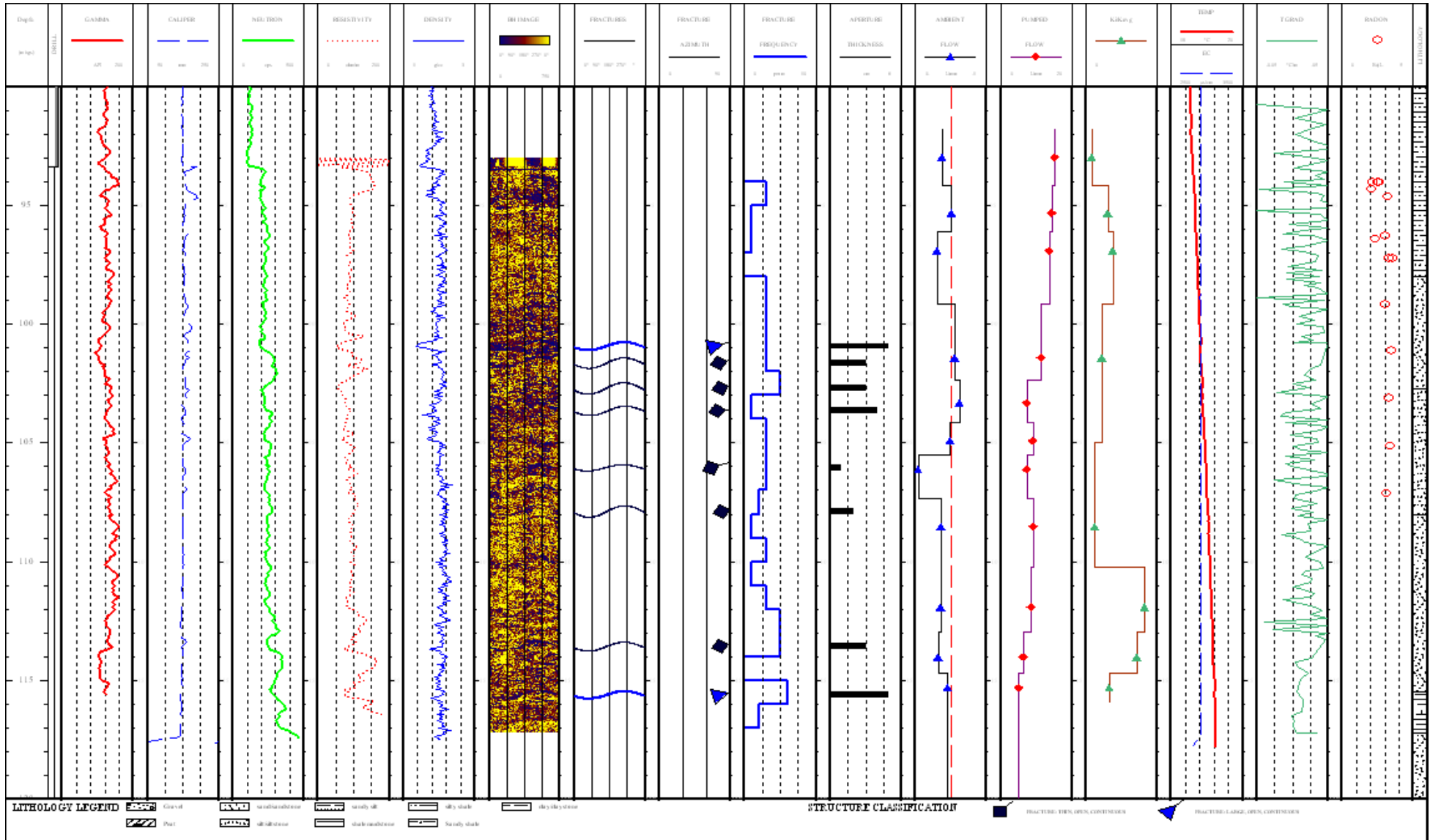


Figure 4.2 Composite geophysical logs for BH3

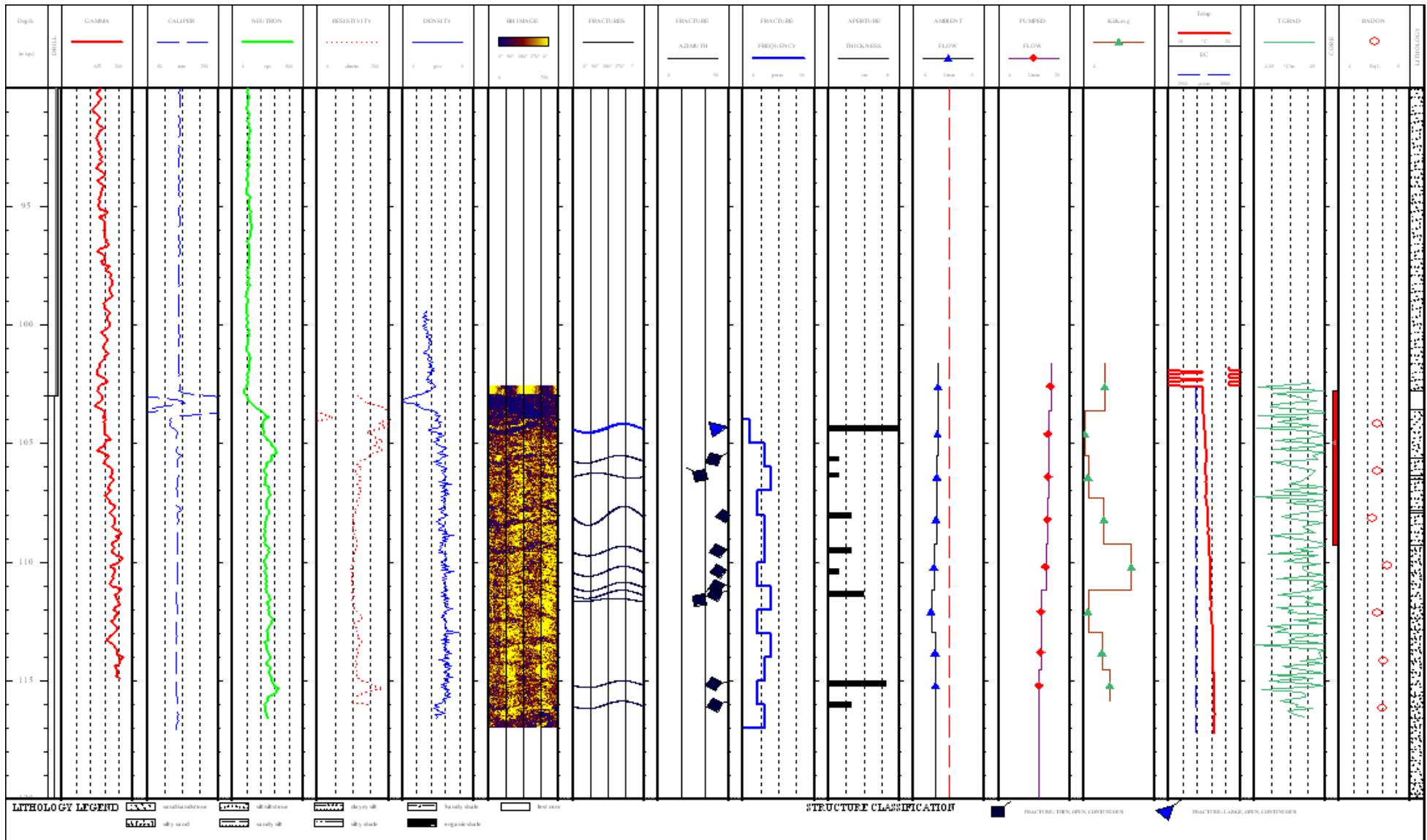


Figure 4.3 Composite geophysical logs for BH4

4.3. Downhole Electromagnetic Flowmeter (EMF) Logging

4.3.1. Principles of the EMF

A downhole electromagnetic flowmeter (Quantum Engineering Corporation, TN, USA) was used to measure vertical flow rates within the well, from which relative hydraulic conductivity (K/K_{ave}) profiles are derived. The procedure involves measuring ambient flow rates within the contributing interval(s) of the well and then repeating the measurements at the same depths under pumped conditions that cause water to flow upwards to the pump inlet situated within the cased zone. All the flow through the cross-sectional area of the well at each targeted depth is channelled through the flowmeter fitted with an inflatable packer (Appendix 1C). The difference between the ambient and induced (pumped) flow rates between two adjacent depths gives the net induced flow contribution within that interval (or layer). Since flow paths in the aquifer due to pumping tend to become more horizontal as vertical gradients diminish, the amount of water entering the well during steady-state conditions is directly proportional to the hydraulic conductivity of that interval (Molz *et al*, 1994; Pavelic *et al*, 2006). K/K_{ave} in the horizontal plane for each interval, i , was calculated from the following equation:

$$K/K_{ave} = (Q_i / z_i) / (Q_p / \sum z_i) \quad (1)$$

where Q_i is the net flow contribution, z_i is the thickness of the layer and Q_p is the pumping rate, as derived in Molz *et al.* (1994).

4.3.2. Field testing

The calliper log was run prior to EMF testing to determine the variability in the diameter within the uncased interval from which to identify depths that the flowmeter and packer assembly could be reliably positioned without compromising data quality or the equipment. Nine depths were selected for testing within the exposed formation of BH3 plus one within the cased zone, resulting in an average measurement spacing of 2.7 m. For BH4, seven depths were identified with an average measurement spacing of 2.0 m. Next, EMF measurements were made at the selected depths under ambient (i.e. static) conditions. Finally, the EMF measurements were repeated under induced (i.e. pumped) conditions once quasi steady-state conditions had been reached. To create the induced conditions a Grundfos MP1 monitoring pump was lowered into the cased zone to a depth of about 30 m bgs and operated at a constant rate of around 0.25 L/s. Representative values were collected after the perturbation caused by moving and repositioning the tool had dissipated to the point where the standard deviation between readings was less than the accuracy quoted by the manufacturer (0.02 L/min).

4.3.3. EMF Results

4.3.3.1 Flow profiles

The flow profiles for ambient and induced conditions are presented in Figures 4.2 and 4.3. It should be noted that a positive flow rate is indicative of upward flow in the well (e.g. due to pumping), whilst a negative flow rate indicates downward flow.

Ambient flow rates for BH3 are low (-0.10 to +0.03 L/min) and for BH4 are even lower (-0.04 to -0.03 L/min). This conforms with expectation, given the limited groundwater withdrawal from the basement aquifer and the low hydraulic gradient due to the proximity to the coast. The predominance of downward ambient flow could be indicative of a net contribution towards deeper zones of the aquifer.

Induced flow rates gradually increase toward a value approximating the pumped rate at the top of the formation and within the cased zone. Variations in the flow gradient (Q_i/b_i) are indicative of contrasts in K/K_{ave} as described in the proceeding section.

The contribution at the lowest measureable depth (around one metre from the bottom of the well), was 34% of the pumped flow for BH3 and 78% for BH4, indicating that a significant proportion of the flow arises from lower depths. Given that in both cases this contribution is approximately proportional to the backfilled length of the open interval of the well, it is possible that the slumped interval remains hydraulically active and continues to contribute to flow. If sediment at the base of the well consolidates during injection then access to this zone may not continue during ASR operations.

Since the net flow contribution between successive intervals must either remain unchanged or increase during logging in the ascent mode, the occurrence of 2 out of 3 adjacent measurements that deviate from this trend between depths of around 102 to 107 m bgs for BH3 strongly suggests the occurrence of bypass flow around the packer within this zone. The caliper reveals nothing unusual at these depths, providing evidence that the bypass flow is occurring within the adjacent formation along fractures rather than within the well itself due to incomplete sealing around the perimeter of the packer. Interestingly, the ambient profile also showed the highest flow gradients at a similar depth.

4.3.4. K/K_{ave} profiles

The flowmeter-derived K/K_{ave} profiles are shown in Figures 4.2 and 4.3. The range in hydraulic conductivity observed at BH3 was 10-fold ($K/K_{ave} = 0.25-2.5$) and at BH4 was 29-fold ($K/K_{ave} = 0.07-2.0$). The greater variability of BH4 is most likely reflective of the smaller average spacing of measurements, which conforms with a number of studies that indicate the degree of heterogeneity observed is strongly affected by the scale of measurement. As the resolution of the measurement interval decreases there is less integration over contrasting units and more of the variability is revealed, right down to the smallest measurement scale. This has been demonstrated in both porous media aquifers (Pavelic *et al*, 2006) and hardrock aquifers (Novakowski and Lapcevic, 1999).

Hydraulic conductivity in fractured rock typically varies by around six orders of magnitude (Novakowski and Lapcevic, 1999; Muldoon and Bradbury, 2005; Lemieux *et al*, 2006). Flowmeter-derived K profiles from this study vary by less than two orders of magnitude, and are comparable to similar tests for non-karstic sandy limestone aquifers (Pavelic *et al*, 2006). These data also deviate from the classical fractured rock response in the sense that pumping-induced changes are steady rather than the abrupt discontinuities encountered at individual fractures, which is more indicative of porous media.

4.3.5. Comparison between the well yield testing during drilling and EMF data

Drilling of BH3 was stopped for airlift discharge testing of well yield at three depths within the bedrock aquifer (105, 115 and 125 m bgs). This allowed the relative contribution to the total discharge rate for the three, approximately equal intervals to be calculated and compared to the results from the EMF survey (Table 4.6). The yields were <0.1, 0.7 and 1.5 L/s at the three depths respectively. Recall for comparison that the pumping rate of the EMF tests was around 0.25 L/s.

The airlift test results suggest that the relative flow contribution increases with depth, with the lower two sections of the aquifer substantially higher than the upper section. In contrast, the EMF results suggest the highest contribution occurs within the upper section, with higher uniformity observed between the three intervals. Incomplete development of the well prior to airlift testing of the two uppermost intervals could possibly explain the divergence between the two methods.

Table 4.6 Comparison of percent flow contribution of BH3 between all well yields during drilling and EMF profile

Depth interval (m bgs)	% flow contribution:	
	Drilling	EMF
93–105	<7	41
105–115	40	26
115–125	53	33

4.3.6. Estimated fracture apertures from EMF data

Assuming that fractures can be represented as a planar void between two flat parallel surfaces, then the transmissivity of the aquifer can be used to derive the equivalent fracture aperture thickness by applying the cubic law. This is given by Cook (2003) as:

$$T_f = b^3 \rho g / 12 \mu \quad (2)$$

where T_f is the transmissivity of an individual fracture, b is the fracture aperture, ρ is the density of water, g is acceleration due to gravity and μ is the viscosity of water.

Incremental transmissivities for the eight intervals from each well were determined from the K/K_{ave} (Figures 4.2 & 4.3) and bulk aquifer transmissivity (Table 2.1) data and assumed to equate to T_f from a single fracture occurring in each interval.

Calculated apertures vary from 0.4–2.4 mm overall, with the geometric mean of 1.2 mm for BH3 and 0.8 mm for BH4 (Table 4.7). These values are an upper limit of the aperture of individual fractures since they assume the transmissivity within each interval arises from just a single fracture and that the matrix is impermeable.

Table 4.7 Calculated values of fracture aperture (b) from incremental transmissivities determined from flowmeter and pumping test data

Well	Increment No.	Depth interval (m bgs)	z_i (m)	K/K_{ave}	T_f (m ² /d)	b (mm)
BH3	1	93–95.33	2.33	0.25	0.024	0.70
BH3	2	95.33–96.93	1.60	0.92	0.061	0.95
BH3	3	96.93–101.43	4.50	1.14	0.211	1.44
BH3	4	101.43–108.53	7.10	0.68	0.198	1.41
BH3	5	108.53–111.93	3.40	0.38	0.053	0.91
BH3	6	111.93–114.03	2.10	2.48	0.214	1.45
BH3	7	114.03–115.33	1.30	2.13	0.114	1.17
BH3	8	115.33–127	11.67	0.99	0.476	1.89
BH4	1	102.6–104.61	2.01	0.89	0.050	0.89
BH4	2	104.61–106.41	1.80	0.07	0.003	0.36
BH4	3	106.41–108.21	1.80	0.19	0.010	0.51
BH4	4	108.21–110.21	2.00	0.86	0.048	0.88
BH4	5	110.21–112.11	1.90	2.02	0.106	1.15
BH4	6	112.11–113.81	1.70	0.18	0.009	0.50
BH4	7	113.81–115.21	1.40	0.79	0.030	0.76
BH4	8	115.21–146	30.79	1.11	0.948	2.38

4.4. Acoustic Televiewer Logs

Acoustic televiewer (ATV) logs are widely used to locate and characterise fractures. The tool comprises of an acoustic scanner that uses a rotating, pulsed sound source (magnetometer) and a piezometric transducer for sending and receiving the sound signal to produce a very dense, magnetically oriented, visual image of acoustic reflectivity of the borehole wall and the two-way travel time. Fracture signatures can be identified and the fracture depth, orientation, dip and apparent aperture determined.

The image data from both wells reveal steeply dipping fractures to the E-NE relative to magnetic north (typically 75%), at dip angles that average between 73% and 74% for both wells (Figures 4.2 & 4.3). Fractures typically run parallel to the bedding planes. Dip angle and orientation conform with the regional structure determined by Whiting (1967).

In BH3, eight large continuous fractures are identified at depths of 100.9 m, 101.6 m, 102.7 m, 103.7 m, 106.0 m, 107.9 m, 113.6 m and 115.6 m. In BH4, nine large continuous fractures occur at 104.4 m, 105.6 m, 106.3 m, 108.0 m, 109.5 m, 110.4 m, 111.3 m, 115.1 m and 116.0 m. Apparent aperture thicknesses vary from 10 to 50 mm in BH3 and from 10 to 100 mm in BH4. Other smaller, discontinuous fractures occur at densities ranging from 0 to 6 per metre in BH3 and from 1 to 4 per metre in BH4. Since the vertical resolution of the acoustic scanner tool is quoted to be around 1 mm, only macro-scale features can be detected. ATV fractures apertures are 1–2 orders of magnitude larger than that determined from the EMF data based on the cubic law analysis, and a similar order greater than typical values for fractured rock aquifers (Cook, 2003).

Comparing the ATV logs and temperature gradient profiles indicates that at three of the five depths in BH3 and at only one of four depths in BH4 did the temperature anomaly coincide with fractures identified from the ATV logs.

4.5. Radon Profiles

Radon concentrations range from 2.1–3.6 Bq/L in BH3 and from 2.3–3.4 Bq/L in BH4. Radon concentrations in BH3 exceed BH4 over the three depth increments with overlapping measurements from 104–107 m. This is suggestive of higher groundwater velocities at BH3 which concurs with the slightly higher transmissivity value determined for that well. Differences in radon concentration within a well exceed the differences between wells, which could also be driven by varying source concentrations as a result of aquifer heterogeneity.

4.6. Well Stability

Lennon *et al* (2006) expressed caution regarding the stability of the target formation for an uncased (open-hole) completion and this issue warrants consideration here. This concern is reinforced by evidence of slumping in the lower sections of both investigation wells and the detection of high particulate concentrations in the extracted waters during pumping.

As previously stated, the total depths of BH3 and BH4, as measured on 21–22 June 2006, were 9 m and 29 m less than the total drilled depths respectively. BH3, the more productive of the two wells (Table 2.1), was selected for reaming operations. The change in the total depth and diameter of BH3 as a result of the development is clearly illustrated in Figure 4.4. The depth was increased from 117.1 m to 123.5 m, but still remained 3.5 m short of the reamed depth of 127 m bgs (i.e. the original drilled depth).

The development increased the average effective diameter of the well from 152.7 mm to 163.3 mm over the common depth interval of 93.1 m to 117.1 m. The expansion in well diameter was not uniform, with differences before and after reaming ranging from -15mm to +123 mm (Figure 4.4). The three most pronounced zones of erosion were from 93–95 m, 99–106 m and 115–116 m, with a clear bias towards the upper half of the formation. In contrast, the regional study by Leonard (1992) indicates the lower rather than the upper part

of the bedrock aquifer is more highly weathered. The zones of greatest erosion include both of the lithologic classes (Figures 4.2 & 4.3) and may be most susceptible to future erosion. No significant correlation was observed between the change in well dimensions and the corresponding natural gamma count, reaffirming that lithology was not the major influence on the stability of the formation.

The quantity of sediment that would have been recovered to account for the 11 mm increase in well diameter (7% increase in well volume) may be easily calculated at 150 kg for the measured bulk density value of 2.3 g/cm³ (Table 4.3). This appears reasonable from observations of quantity of sediment recovered from the well.

Erosion of the weathered bedrock sediments produced high particulate concentrations in the extracted water. During pump testing, Lennon *et al* (2006) reported that TSS levels in the extracted groundwater were around two orders of magnitude higher in BH3 compared to BH4. Values for BH3 commenced at 150 mg/L, declining to 64 mg/L by the end of the test; whilst for BH4, TSS values were initially 2 mg/L and declined to < 1 mg/L. Lennon *et al*, (2006) proposed that the additional 10 m of open interval between 93 m and 103 m consisting of highly weathered bedrock (that had been cased-off in BH4) may have been mobilised during pumping. This is largely supported by the data presented in Figure 4.4, which indicates that this interval was responsible for much (although not all), of the increase in well diameter due to the reaming operation of 23 June.

The high particulate concentrations observed in BH3 constitute a risk to ASR as a result of mechanical clogging caused by particle mobilisation and redeposition. Before injection commences this well should be developed by high rate pumping or air jetting until TSS levels are reduced to those comparable to BH4; notionally <5 mg/L.

If water treated by reverse osmosis was injected it is expected that dispersion may occur in some layers, however stormwater at the salinity tested unlikely to contribute to dispersion, and hence clogging or well instability.

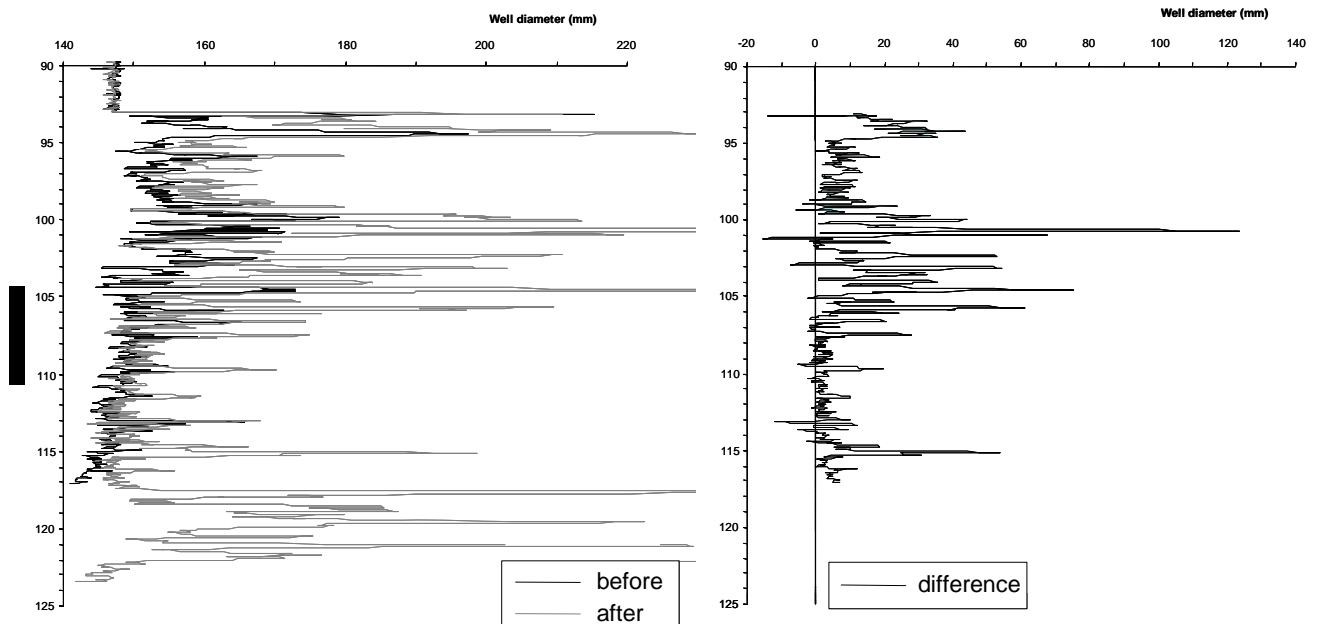


Figure 4.4 Caliper logs of BH3 well before and after well development (left), and the resultant difference in well diameter (right)

5. DISCUSSION

Examination of the core samples suggested that most of the flow in the aquifer would be derived from the sandstone due to its higher fracturing and higher matrix permeability. However at field scale this appeared to not necessarily hold true as the degree of weathering within the aquifer and subsequent location, density and interconnectedness of fractures appeared to be the main factor controlling groundwater inflows.

The EMF results indicate little or no consistency in the K/K_{ave} profiles between the two wells, and no general image emerges when the two profiles are compared, apart from the aquifer appearing to be a succession of alternating sequences of high and low hydraulic conductivity, of a thickness typically less than the 2–3 m measurement scale.

Comparison of the K/K_{ave} profiles with the distribution of fractures identified from the ATV logging suggests some correlation between fracture occurrence and hydraulic conductivity. For BH3, the two main fracture zones (100–107 m and 113–115 m) also conform with higher values of K/K_{ave} . Effective fracture apertures are estimated to be far smaller than suggested from the ATV data, implying that most of the fractures are hydraulically inactive.

Radon data also lend support to the EMF data, with radon concentrations positively correlated to K/K_{ave} data in both wells, with R^2 values of 0.37 for BH3 and 0.43 for BH4.

From the above it can be seen that a useful and reliable characterisation of the Silurian aquifer is difficult to achieve from any of the characterisation methods individually, but may be gained by an approach that combines various methods used.

6. CONCLUSIONS

The target aquifer may be classified as a dual-porosity fractured rock with small fracture apertures and relatively high matrix porosities and low matrix permeability. In light of the moderate degree of variability in K/K_{ave} profiles, and the general absence of distinct signatures in the temperature gradient and radon concentration profiles, it would appear that the aquifer exhibits either a low degree of aquifer heterogeneity, or more likely, heterogeneity at scales less than the scales of measurement.

Given the apparent low degree of aquifer heterogeneity, combined with the low hydraulic conductivity and low hydraulic gradients and brackish groundwater salinity, if this behaves as a single-porosity aquifer ASR operations are unlikely to be impinged by low recovery efficiencies (Pavelic *et al*, 2006). However, the dual-porosity characteristics of the target aquifer, and particularly the degree of dispersive and diffusive interaction between the low salinity recharge water migrating along fractures with the high salinity ambient groundwater, would imply a lower recovery efficiency (Wright and Barker, 2001). Ultimately, verification would require conducting cycle testing during the field trial.

The Silurian aquifer has been shown to be susceptible to erosion, which, under an ASR scenario, could cause mobilisation and recovery of aquifer fines (note that the weathering of siltstone mobilises clay and weathering of sandstone mobilises sand). Clay dispersion tests reveal that no significant dispersion was observed for either mains water or stormwater relative to that of the ambient groundwater. In contrast, distilled water had higher dispersive potential that was reasonably correlated with the CEC of the aquifer samples. Without amendment, water of this quality should not be injected into the Silurian aquifer.

The low transmissivity, small fracture apertures and small pore sizes in the matrix suggest a high potential for clogging unless the stormwater injectant is treated to near-potable standards. Water quality data from related investigations currently in progress indicate that the injection of oxygenated potable water into the anaerobic aquifer that contains an abundance of iron minerals (e.g. pyrite, siderite) could lead to clogging by precipitation of iron oxides, which would require routine backwashing and possibly more rigorous treatments such as acidisation (Pérez-Paricio and Carrera, 1999).

7. RECOMMENDATIONS

ASR into the weathered bedrock aquifer at Rossdale is not without risk and should only proceed with caution.

1. The low well yields for both investigation wells suggest injection rates of <1 L/s; probably around 0.5 L/s. This rate, as previously identified, is too low to provide an ASR operation with cost of recovered water less than the current cost of mains water, taking into account capital and operating costs. If ASR is to proceed at the Rossdale site, it would be from the viewpoint of serving as a site to demonstrate the potential for stormwater ASR in Melbourne, recognising that this site is at the most difficult end of the spectrum of sites considered. In that sense, success at Rossdale would give confidence for ASR elsewhere in Melbourne, but failure would not preclude ASR from succeeding elsewhere.
2. BH3 is the most productive of the two investigation wells and the more prospective to serve as the ASR well. BH4, situated 11 m from BH3, would therefore serve as an observation well.
3. Prior to initiating the ASR trial, further development of BH3 is required to reduce TSS levels in extracted water to <5 mg/L, as has been achieved for BH4. If BH3 cannot be stabilised, then BH4 should be used as the ASR well and BH3 used as an observation well.

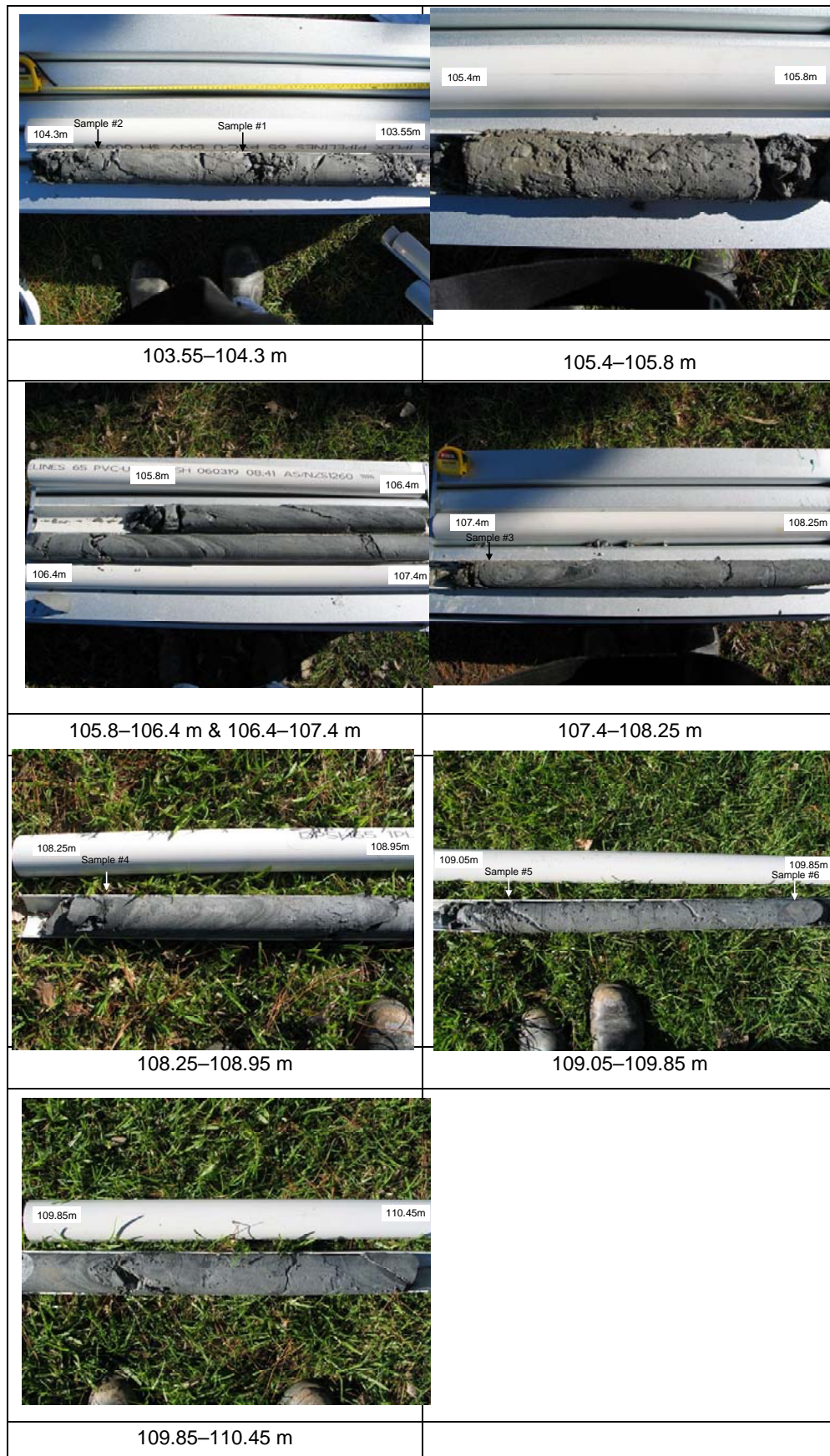
8. REFERENCES

- Blatt, H., Middleton, G. and Murray, R. (1980) Origin of sedimentary rocks. 2nd Ed. Prentice-Hall Inc., Englewood Cliffs, New Jersey.
- Brown, D.L. and Silvey, W.D. (1977) Artificial recharge to a freshwater-sensitive brackish-water sand aquifer, Norfolk, Virginia, U.S. Geol. Survey Prof. Paper 939.
- Cook, P.G., Dighton, J.C. and Love, A.J. (1999) Inferring ground water flow in fractured rock from dissolved radon. *Ground Water* 37(4):606-610.
- Cook, P.G. (2003) A guide to regional groundwater flow in fractured rock aquifers. CSIRO and Land and Water Australia Report, ISBN 1 74008 233 8.
- Cook, P.G., Lamontagne, S., Berhane, D. and Clark, J.F. (2006) Quantifying groundwater discharge to Cockburn River, southeastern Australia, using dissolved gas tracers 222Rn and SF6. *Water Resources Research* 42, W10411, doi:10.1029/2006WR004921.
- Gray, D.H. and R.W. Rex (1990) Formation damage in sandstones caused by clay dispersion and migration. In: Bailey S.W. [Ed.], *Clay and Clay Minerals Conference Proceedings, 14th National Conf. Clays Clay Mineralogy*, 120(14):355-366 Published by Pergnon London, 1966. Formation Damage, SPE Reprint Series No. 29, 82-95.
- Hess, A.E. (1986) Identifying hydraulically conductive fractures with a slow-velocity borehole flowmeter. *Can. Geotech. J.* 23:69-78.

- Konikow, L.F., August, L.L. and Voss, C. I. (2001) Effects of clay dispersion on aquifer storage and recovery in coastal aquifers. *Transport in Porous Media* 43:45–64.
- Leonard, J.G. (1992) Port Phillip region groundwater systems - future use and management. Department of Water Resources, Victoria.
- Lemieux, J.-M., Therrien, R. and Kirkwood, D. (2006) Small scale study of groundwater flow in a fractured carbonate-rock aquifer at the St-Eustache quarry, Québec, Canada. *Hydrogeology Journal* 14:603-612.
- Lennon, L., Parsons S. and Dudding M. (2006) Developing aquifer storage and recovery (ASR) opportunities in Melbourne: hydrogeological assessment for an ASR trial site (Rossdale Golf Club). Report prepared by Sinclair Knight Merz for the Victorian Smart Water Fund with support from CSIRO Water for a Healthy Country Flagship Program.
- Molz, F.J., Boman, G.K., Young, S.C. and Waldrop, W.R. (1994) Borehole flowmeters: field application and data analysis. *Journal of Hydrology* 163:347-371.
- Muldoon, M. and Bradbury, K.R. (2005) Site characterization in densely fractured dolomite: comparison of methods. *Ground Water* 43(6):863-876.
- Novakowski, K. S. and Lapcevic, P. A. (1999) Development of a conceptual model for ground flow and contaminant transport in a horizontally-stratified carbonate rock using detailed hydraulic testing results. *Contaminated Site Remediation: Challenges Posed by Urban and Industrial Contaminants* (Ed. C.D. Johnston). Proc. 1999 Contaminated Site Remediation Conference, Fremantle, Western Australia, 21-25 March 1999, pp.149-156.
- Pavelic, P., Barber, C., Dillon, P., Toze, S. and Yin Foo, D. (2001) Water banking trial at Waruwi, South Goulburn Island, NT. Stage 1 Report to Department of Land Planning and Environment, Northern Territory. Centre for Groundwater Studies Report No. 98.
- Pavelic, P., Dillon, P.J. and Simmons C.T. (2006) Multi-scale characterization of a heterogeneous aquifer using an ASR operation. *Ground Water* 44(2):155-164.
- Pérez-Paricio, A. and Carrera, J. (1999) *Clogging Handbook*. EU Project on Artificial Recharge of Groundwater, Research program on Environment and Climate, Contract ENV-CT95-0071.
- Scheuerman, R.F. and Bergersen, B.M. (1990) Injection water salinity, formation pretreatment, and well operation fluid selection guidelines. In: *Formation Damage*, SPE Reprint Series No. 29, pp.155-170.
- Standards Association of Australia (1980) Determination of Emerson Class Number of a Soil. AS 1289.C8.1.
- Whiting, R.G. (1967) General geology of the Melbourne area. 3-1. Silurian: structure and stratigraphy. In: *Geology of the Melbourne district*. Geological Survey of Victoria. Bulletin No. 59.
- Wright, T.E.J. and Barker, J.A. (2001) Calibration of a dual-porosity solute transport model using short and long term tracer tests. Proc. IAH XXXI Congress, 'New Approaches to Characterising Groundwater Flow', Munich, Sept. 2001, Vol. 1, pp.683-688.

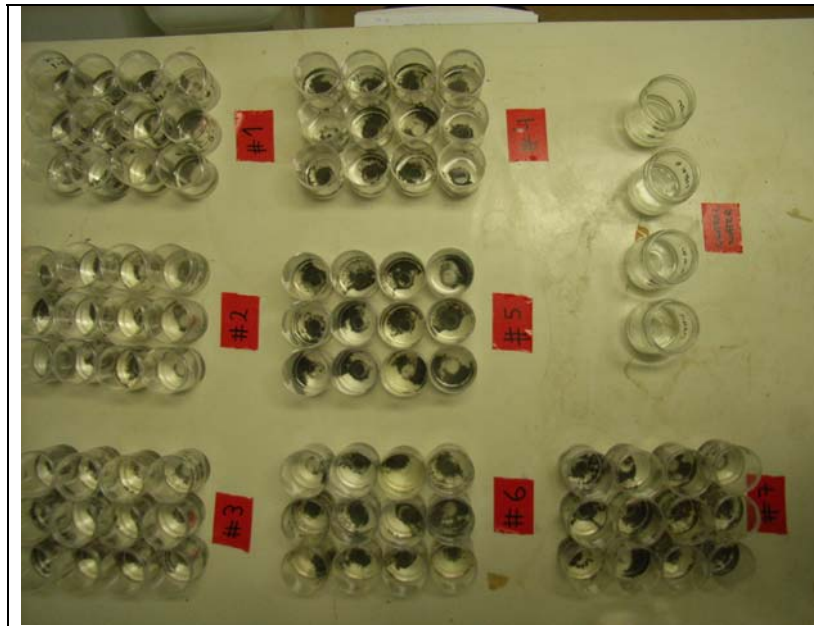
APPENDIX 1: SELECTION OF PHOTOGRAPHIC IMAGES

A. Intact core samples from BH4 (Source: Stephen Parsons, SKM)



B. Other images of aquifer material

<p>Core sample from BH4 following oven drying. Note the partitioning of the core along a bedding plane due to handling following oven-drying.</p>	<p>Pyrite nodules extracted from BH3 during reaming operation shown below.</p>



Clay dispersion tests of 7 aquifer samples and 4 water types, plus controls (water only). All tests were performed in triplicate

<p>Low dispersing sample #1 with mains water</p>	<p>Relatively high dispersing sample #6 with distilled water</p>

C. Well construction and testing



Reaming operations in BH3 performed by Romano Grande (Borewell Pty Ltd) on the morning of 23 June 2006.



EMF testing of BH4. Don Freebairn (DWLBC) is shown lowering the flowmeter and packer assembly down the well. Two reels containing the pressure delivery tubing and monitoring pump can be seen on the bottom RHS of the image.



Paul Kortholt (RGC) is shown recovering the diffusion chambers from BH4. Note the black precipitous depositions indicative of highly anaerobic conditions (no such deposits were observed in BH3).



Contact Us

Phone: 1300 363 400

+61 3 9545 2176

Email: enquiries@csiro.au

Web: www.csiro.au

Your CSIRO

Australia is founding its future on science and innovation. Its national science agency, CSIRO, is a powerhouse of ideas, technologies and skills for building prosperity, growth, health and sustainability. It serves governments, industries, business and communities across the nation.